Available online at website: https://journal.bcrec.id/index.php/bcrec

Bulletin of Chemical Reaction Engineering & Catalysis, 19 (2) 2024, 230-241

Research Article

A Facile and Rapid Immobilization Method of Titanium Dioxide-Alginate Composite for the Photocatalytic Removal of Reactive Black-5

Weng Hoong Lam[1,2,3,*], Lee Hong Tee[1,2], Zhen Hong Ban[1,2]

[1]School of Energy and Chemical Engineering, Xiamen University Malaysia, Jalan Sunsuria, Bandar Sunsuria, 43900 Sepang, Selangor, Malaysia.
[2]College of Chemistry and Chemical Engineering, Xiamen University, Xiamen 361005, China.
[3]Center of Excellence for NaNo Energy & Catalysis Technology (CONNECT), Xiamen University Malaysia, Sepang, Selangor, 43900, Malaysia.

Received: 21st February 2024; Revised: 12th April 2024; Accepted: 15th April 2024
Available online: 24th April 2024; Published regularly: August 2024

Abstract

A facile and rapid approach to immobilize nano-sized titanium dioxide (TiO_2) using a renewable biopolymer (i.e. alginate) has been successfully demonstrated. TiO_2 exhibits a positively charged surface in acidic environment due to the presence of hydroxyl groups. Meanwhile, alginate polymer is negatively charged at any pH due to the presence of carboxylic group in the polymer chain. The negatively charged alginate polymer and positively charged TiO_2 formed composite instantaneously when the alginate polymer was introduced into the TiO_2 nanoparticles suspension. The TiO_2-alginate (TiO_2-A) composite photocatalyst was characterized using thermogravimetric analysis (TGA), field emission-scanning electron microscopy (FE-SEM) coupled with energy dispersive X-ray (EDX) analysis and Fourier Transform Infrared (FTIR). Thermogravimetric analysis indicated that incorporating TiO_2 into sodium alginate increases its decomposition temperature due to the stability of TiO_2 at elevated temperatures, with the TiO_2 content estimated in the composite being 55.6%, lower than the theoretical calculation of 62.8%. FTIR analysis revealed a shift in the peak of the carboxylic group of sodium alginate, suggesting composite formation through electrostatic interactions with TiO_2 nanoparticles, while FESEM analysis showed that the TiO_2-A composite surface exhibited more pores compared to protonated alginate. The TiO_2-A composite was able to remove 90% of the Reactive Black 5 (RB5) in less than 200 min under Ultra-violet (UV) illumination. The optimal pH to remove RB5 was found to be pH 2 due strong electrostatic attraction of negatively charged RB5 on the positive surface of TiO_2 nanoparticles. The photocatalyst can be recovered by simple separation method, i.e. gravitational settling, and reused for 10 consecutive cycles with efficiency greater than 90% consistently. The TiO_2-A composite is a promising immobilized photocatalyst for practical application in wastewater treatment.

Keywords: Alginate; TiO_2; Biopolymer; Rapid immobilization; Photocatalyst

How to Cite: W.H. Lam, L.H. Tee, Z.H. Ban (2024). A Facile and Rapid Immobilization Method of Titanium Dioxide-Alginate Composite for the Photocatalytic Removal of Reactive Black-5. *Bulletin of Chemical Reaction Engineering & Catalysis*, 19 (1), 230-241 (doi: 10.9767/bcrec.20133)

Permalink/DOI: https://doi.org/10.9767/bcrec.20133

1. Introduction

TiO_2 possesses distinctive electronic and structural properties that make it an effective photocatalyst [1,2]. The utilization of nano-sized semiconductor titanium dioxide (TiO_2) photocatalysts in water purification has garnered great interest due to its proven efficiency in the mineralization of recalcitrant organic pollutants without producing secondary pollutants. The capability of TiO_2 in the degradation of various organic compounds under Ultra-violet (UV) irradiation, including different types of dyes has

* Corresponding Author.
Email: wenghoong.lam@xmu.edu.my (W.H. Lam)

been well documented [3,4]. However, the practical realization of heterogeneous photocatalysis using nano-sized TiO_2 in current water treatment practices has been hindered by the high cost involved in separating the TiO_2 nanoparticles suspended in treated water sources [5].

While high photoactivity of photocatalysts is often desired, the ease of recovery of the photocatalyst and their reuse are of equal importance in practical applications. Numerous methods to recover TiO_2 nanoparticles from bulk solution were reported in the literature including coagulation [6], filtration [7], and centrifugation [8]. However, these methods are limited by some constraints. For example, coagulation requires the addition of coagulants post-water treatment and the process to re-suspend the TiO_2 particles is difficult; a filtration system causes the clogging of filter pores, thus rapid backwashing is often needed; centrifugation is costly and is only suitable for lab-scale operation. In order to resolve the post-separation issue of fine TiO_2 particles used in water treatment, many researchers have attempted to immobilize nano-sized TiO_2 particles onto fixed supports, such as: glass, activated carbon [9], silica [10,11], zeolites [12,13], clay [14,15], and polymer substrates, such as: polystyrene [16] and polyethylene terephthalate (PET) [17], and others [18]. These supports are predominantly sourced from non-renewable origins, leading to significant environmental implications.

Among various support options, sustainable and renewable supports are prioritized for their environmentally friendly characteristics and sustainability. Alginate stands out as a prime example in this category [19,20]. Derived from marine brown algae, alginate is a natural, anionic polymer abundant in nature, making it an ideal choice for environmentally conscious applications. Recently, the immobilization of semiconductor photocatalysts in renewable natural or biopolymers, such as alginate, has received increasing interest [21–23]. Additionally, these biopolymers have advantage over the conventional TiO_2 supports because most renewable biopolymers are light transparent material, thus suitable for TiO_2 immobilization since photocatalysis involves light activated reaction step.

Conventionally, TiO_2 nanoparticles can be immobilized in biopolymer beads using an extrusion-dripping method [24–26]. In this case, the nano-sized TiO_2 particles are mixed with the polymeric sol and subsequently extruded dropwise through a nozzle into a hardening bath, forming beads with entrapped TiO_2 nanoparticles. This method has very low immobilization productivity due to the drop-wise generation of polymer particles. Furthermore, the size of the particles form is in millimetric size (approx. 2 mm) and not very suitable as photocatalyst.

In this study, we investigated a one-step facile and rapid immobilization method for immobilizing TiO_2 nanoparticles, a potent photocatalyst, using a sustainable and renewable natural polymer, alginate by making use of the electrostatic interactions of the nanoparticle and biopolymer. An ideal immobilization process should be both easy and quick, achievable under ambient conditions using simple equipment. The focus of this work was on developing a rapid immobilization process to form TiO_2-alginate (TiO_2-A) composite photocatalyst using TiO_2 nanoparticles and alginate polymer. The immobilization process reported is facile because the process only involves dispersing the TiO_2 nanoparticles in alginate polymeric sol at ambient conditions. Additionally, the process is rapid due to the instantaneous electrostatic interaction of negatively charged alginate polymer and the positively-charged TiO_2 nanoparticles, resulting in the formation of TiO_2-A composite. The photoactivity of the TiO_2-A composite was assessed by using Reactive Black 5 (RB5), a common azo dye in the textile industry, as the surrogate organic pollutant. Furthermore, the recoverability and reusability of TiO_2-A composite were also examined.

2. Materials and Methods

2.1 Materials

Sodium alginate (Manugel GHB) powder was obtained from FMC Biopolymers, UK. TiO_2 nanoparticles suspension (anatase, 4-8 nm, 20 wt. %) stabilized by nitric acid (HNO3) was supplied by PlasmaChem GmbH, Germany. Reactive Black 5 (Dye content 55%) was purchased from Sigma Aldrich, Malaysia.

2.2 Preparation of the TiO_2-A Composite Photocatalyst

TiO_2-A composite was prepared by adding 20 mL of sodium alginate solution (20 g/L) into 400 mL TiO_2 nanoparticle suspension (0.2 wt. %) agitated under a constant stirring speed of 2500 rpm. The sodium alginate solution was prepared by dissolving 2 g of sodium alginate powder in 100 mL of deionized water. Upon addition of sodium alginate solution into the TiO_2 nanoparticle suspension, TiO_2-A composite was formed instantaneously. The TiO_2-A composite in the suspension was allowed to stir at 2500 rpm for another 30 min before the stirring was stopped. The TiO_2-alginate composite was left to settle overnight. The immobilization process is shown in Figure 1.

2.3 Characterization of the TiO_2-A Composite Photocatalyst

2.3.1 Thermogravimetric analysis (TGA)

A thermogravimetric analyzer (TA Instruments, Q50) was used to study the thermal stability of TiO_2-A composite and to estimate the amount of TiO_2 loaded onto the TiO_2 A composite. The decomposition profiles of dry TiO_2-A composite and dry sodium alginate powder were recorded with a heating rate of 10 °C/min between room temperature to 1000 °C under purified air at a flow rate of 100 mL/min.

The amount of TiO_2 (dry mass basis) present in the TiO_2-A composite was determined by determining the residual mass after the TiO_2-A composite sample was oxidized in air under elevated temperature. The composition of TiO_2 nanoparticles immobilized in TiO_2-A composite was estimated using Equation (1).

$$TiO_2 \text{ content } (\%) = \left[\frac{m_{TiO_2-A,1000°C}}{m_{TiO_2-A,100°C}} - W_{SA}\left(\frac{m_{SA,1000°C}}{m_{SA,100°C}}\right)\right]\times 100\% \quad (1)$$

where, W_{SA} is the mass ratio of sodium alginate to total solid content (sodium alginate and TiO_2 nanoparticles) present, $m_{TiO_2-A,100°C}$ and $m_{TiO_2-A,1000°C}$ are the mass percent of TiO_2-A composite at 100 °C and 1000 °C, $m_{SA,100°C}$ and $m_{SA,1000°C}$ are the mass percent of sodium alginate at 100 °C and 1000 °C. The mass percents of sodium alginate and TiO_2-A composite at 1000 °C were normalized to the respective mass percents at 100 °C to minimize the effect of moisture content on the estimation of TiO_2 composition on TiO_2-A composite.

2.3.2 X-ray Diffraction (XRD)

The crystallinity of alginate and TiO_2-A composite were characterized by XRD. The samples were mounted onto a flat surface and analyzed using a Bruker D8 Discover X-ray diffractometer operated at 40 kV and 40 mA, over the diffraction angle range (2θ) of 5–80°. The samples were scanned at a rate of 0.02° s^{-1} using a Cu-Kα radiation (λ = 1.5406 Å) as the X-ray source.

2.3.3 Particle size analysis

The particle size analysis and the size distribution were carried out using a particle size analyzer (Mastersizer 3000, Malvern Instruments, UK) using laser diffraction. Deionized water was added as the dispersant at a stirring speed of 200 – 800 rpm. An aliquot of 5 mL TiO_2-A composite dispersed in deionized water was introduced in the Hydro-EV sampling accessory and the light intensity was measured using blue and red light and the size distribution of the composite was recorded.

2.3.4 Fourier Transform Infrared Spectroscopy (FT-IR)

A FT-IR spectrometer (Nicolet iS10, Thermo Scientific) was used to characterize the TiO_2 nanoparticle suspension, TiO_2-A composite, and sodium alginate powder (blank sample). An attenuated Total Reflectance sampling accessory (Smart iTR) with a wavenumber cut-off of 650 cm^{-1} was used to analysis analyze the samples. A

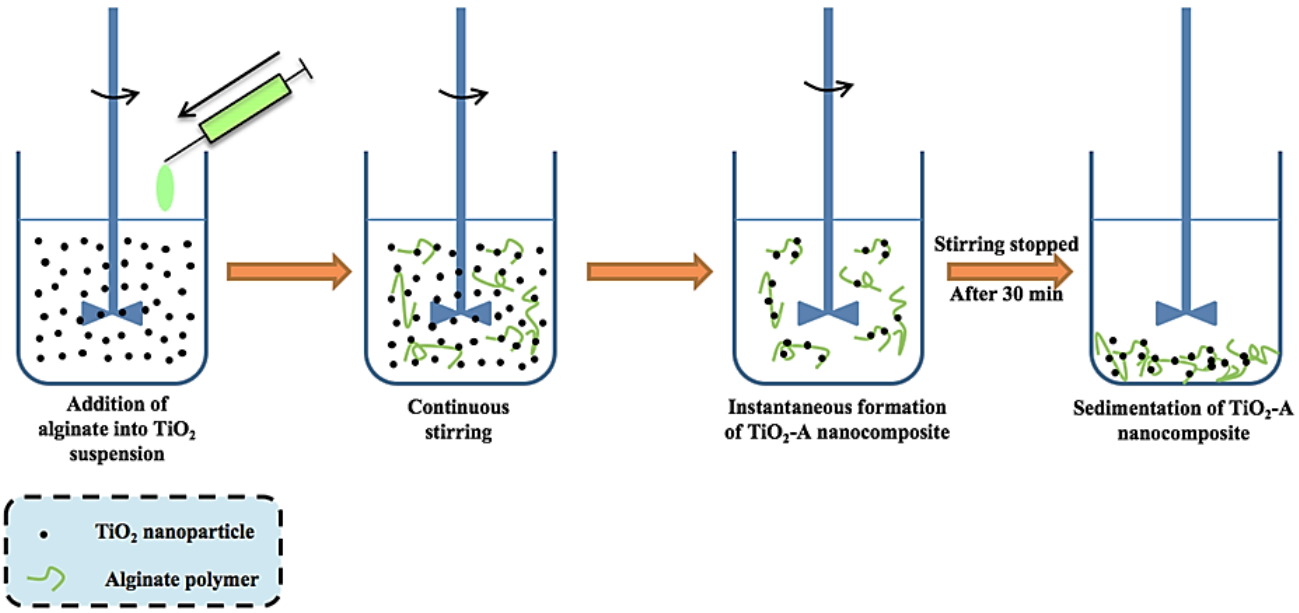

Figure 1. Preparation of TiO_2-A composite.

software (OMNIC Spectra Software Suite) was used to record the spectra of the samples. Each spectrum was constructed from the average of 16 spectra recorded from the sample through a range of 650 to 4000 cm^{-1}.

2.3.5 Field emission scanning microscopy (FE-SEM)

The TiO_2-A composite and protonated alginate were freeze-dried before being mounted on aluminum stubs using double-sided adhesive carbon tape before the samples were observed under the FE-SEM (SU8010, Hitachi). The surface morphology of the composite was examined under FE-SEM with an acceleration voltage of 1.0 – 5.0 kV depending on magnification. The magnifications of 7 – 9 k were selected for low magnification image and the magnifications of 100 – 150 k were selected for high magnification image. Elemental Dispersive X-ray (EDX, SU8010, Hitachi) at an acceleration voltage of 15 kV was also performed to examine the chemical elements present on the surface of the composite. The elemental map of titanium (Ti) was acquired.

2.4 Photoactivity of the TiO_2-A composite

2.4.1 Experimental Setup

Batch photocatalytic experiments were conducted in an enclosed cabinet using a top-mounted UV light source (Kintons, I_ZUV, 2 × 9 Watt). A 250 mL beaker containing dye solution was placed directly below the UV light source (Approx. 254 nm). The solution was stirred at 800 rpm using a magnetic stirrer (IKA, Germany). The distance between the UV light source and the water level in the 250 mL beaker was maintained at 10 cm in all experiments. The volume of the dye solution used in all experiments was maintained at 220 mL.

2.4.2 Photodegradation of RB5

A fixed initial RB5 concentration of 5 ppm across all experiments. The amount of TiO_2-A composite used in all experiments was maintained at 0.01 % (w/v). At every 30-min interval of irradiation time, 1 mL of dye solution was withdrawn and subjected to centrifugation using a micro-centrifuge (Labogene, Scanspeed mini) at 6000 rpm for 5 min to isolate the TiO_2-A composite from the sample, allowing for the determination the RB5 concentration.

The absorbance RB5 solution the was measured using a microplate reader (Tecan, Sunrise) with temperature maintained at 25 °C with an excitation filter set to 598 nm. RB5 concentration was determined using a calibration curve relating RB5 concentration to absorbance. Concentrations reported in this study are normalized to the initial concentration (C/C_o). Additionally, the effects of pH of the RB5 photodegradation were investigated from a range of pH = 2 to pH = 8. The pH of the RB5 solutions was adjusted using 5 M HCl or 10 M NaOH solution.

2.5 Recovery and Reusability of the TiO_2-A Composite Photocatalyst

After the photocatalytic experiment, the TiO_2-A composite was recovered by gravitational sedimentation for 24 h. Optical images were captured to observe the sedimentation of the photocatalyst. To study the reusability of the TiO_2-A composite, the photocatalyst was left to settle for 24 h before it was reused for another process cycle. This process was repeated for 10 cycles. For each cycle, the removal efficiency of RB5 by the TiO_2-A composite was determined after 4 h of photocatalysis.

3. Results and Discussion

3.1 Characterization of the TiO_2-A Composite

The thermal stability of TiO_2-A composite and sodium alginate is shown in Figure 2. The sodium alginate sample was found to undergo a 3-step mass loss before reaching a constant mass under elevated temperatures. The 3 major mass losses could be associated with dehydration, the decomposition of alginate, and the formation of sodium carbonate (Na_2CO_3) and residual carbonaceous material [27]. For the TiO_2 nanoparticles suspension, the major mass loss at temperatures up to 148 °C could be attributed to the dehydration of the suspension. A slight mass loss was observed from 148 to 400 °C, possibly due to the loss of chemisorbed water molecules [28].

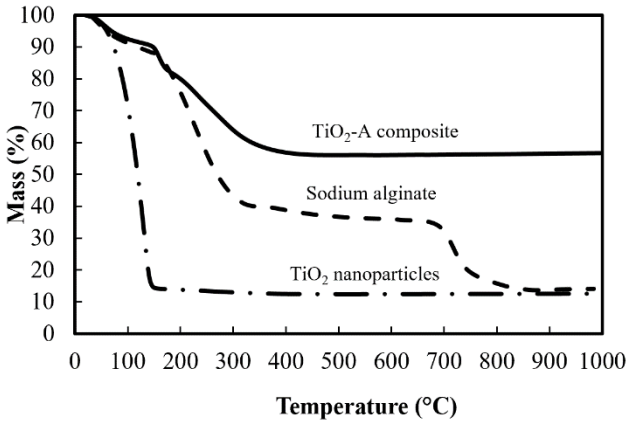

Figure 2. Thermogram of sodium alginate, TiO_2 nanoparticle suspension, and TiO_2-A composite under airflow at elevated temperature.

The first major mass loss of TiO_2-A composite was at 132 °C as compared to the sodium alginate at 160 °C. The incorporation of TiO_2 nanoparticles could have lowered the decomposition temperature of sodium alginate due to the loss of chemisorbed water from TiO_2 nanoparticles in the TiO_2-A composite. The mass of the TiO_2 nanoparticles remains relatively constant from 400 °C to 1000 °C, suggesting a high stability of TiO_2 nanoparticles at elevated temperatures. Additionally, the residual mass of the sodium alg inate from 800 °C to 1000 °C is relatively constant and is mainly contributed by Na_2CO_3 and carbonaceous residuals. From the thermogram of TiO_2-A composite, the mass remained constant from 400 °C to 1000 °C and could be contributed by the residual mass of TiO_2, Na_2CO_3, and carbonaceous residual.

The content of TiO_2 was estimated from the thermograms of sodium alginate and TiO_2-A composite using Equation (1). The assumptions made in this estimation are i) sodium alginate was the limiting material in the preparation process and; ii) the mass loss due to the loss of chemisorbed water from TiO_2 is negligible. The TiO_2 content estimated was found to be 55.6% as compared to the theoretical calculation of 62.8%, likely due the losses during immobilization process.

Figure 3 shows the XRD pattern of sodium alginate, TiO_2 nanoparticles and TiO_2-A composite. The diffraction pattern for sodium alginate clearly indicates the amorphous structure of the biopolymer, which was represented by a broad amorphous halo was observed at region around $2\theta = 5^o - 20^o$, followed by a long stretch of diffuse reflection region, consistent with previous studies [29,30]. The spectrum of TiO_2 nanoparticles also demonstrated the typical peaks observed in literature [31]. The XRD pattern of TiO_2 nanoparticles show the presence of characteristic peaks at 2θ values of 25.3°, 37.7°, 38.5°, 47.8°, 53.9°, 54.9°, which corresponds to the (101), (004), (112), (200), (105), (211) crystal planes of the anatase TiO_2, respectively, as reported in literature [31,32]. The XRD pattern confirmed the presence of both alginate and TiO_2 crystalline phases in the TiO_2-A composite. The characteristic peaks of TiO_2 are present in the XRD pattern of TiO_2-A composite, suggesting the successful immobilization of TiO_2 using alginate biopolymer. Nonetheless, these peaks have broaden after the incorporation of alginate, which is essentially a amorphous material.

Particle size analysis was performed on the TiO_2-A composite and the effect of stirring speed on the size of TiO_2-A composite was examined. Figure 4 presents the size distribution of TiO_2 nanoparticles and TiO_2-A composite. The size distribution of TiO_2 nanoparticles had bimodal peaks at 12 and 91 nm. The presence of the bimodal peaks was likely due to the agglomeration of elemental TiO_2 nanoparticles in the suspension. On the other hand, the particle size of TiO_2-A composite was between 2 to 900 µm with the majority of the composite having an average size of approximately 70 µm. The particle size distribution of the TiO_2-A composite obtained was significantly larger than the TiO_2 nanoparticles. This implies that alginate polymers formed complexes with the TiO_2 nanoparticles in the suspension, thus forming TiO_2-A composite of a larger size.

The TiO_2-A composite was formed through electrostatic complexation of alginate and TiO_2 nanoparticles. This cause them to form larger clusters, as illustrated in Figure 4, therefore, resulted in clusters or particles of different sizes. In particle size analysis, Dv90 indicates that 90%

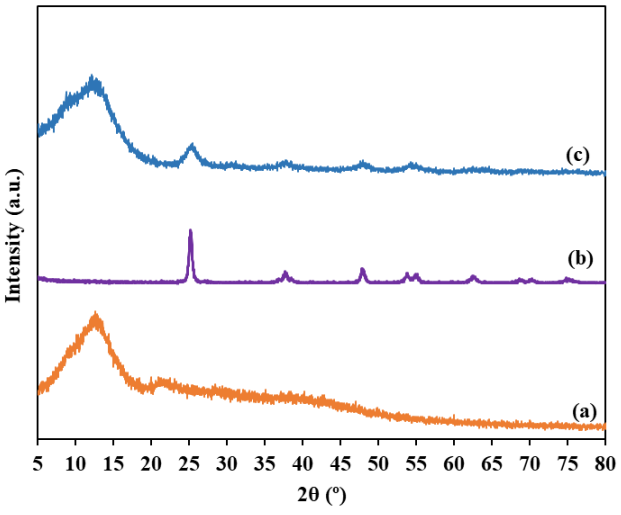

Figure 3. XRD patterns of (a) sodium alginate and (b) TiO_2 nanoparticles and (c) TiO_2-A composite.

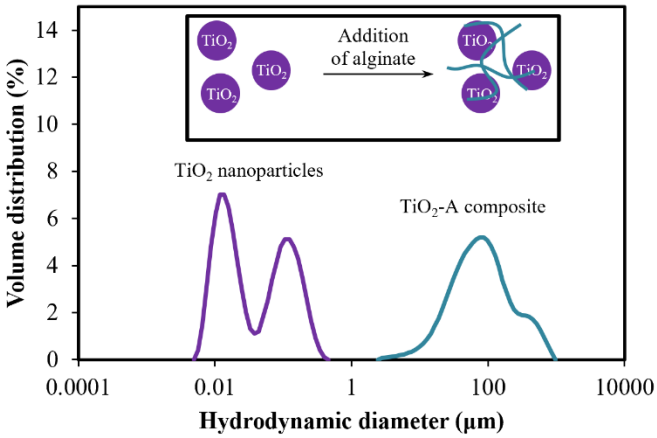

Figure 4. Size distribution of the TiO_2 nanoparticles and TiO_2-A composite. The variation in size is attributed to the formation of TiO_2-A composite (illustration in the subset).

of the particles are smaller than this size, while Dv10 indicates that 10% of the particles are smaller than this size. Since the particle size distribution of the composite follows a normal distribution, the majority of particles, especially the larger ones, are represented by 90% volume, while smaller particles are represented by 10% volume.

Agitation generates shear forces that break down the TiO_2-A composite into smaller sizes. Figure 5 demonstrates that increasing agitation speed leads to a decrease in the hydrodynamic diameters of the composite. The larger composite particles are significantly affected by shear forces, causing them to fragment into smaller sizes. For example, as the agitation speed rises from 200 rpm to 400 rpm, the Dv90 of the composite decreases from 198 to 166 μm, reflecting the breakdown induced by increased agitation. However, at higher agitation speeds (600 to 800 rpm), there are no significant changes in Dv90 size, suggesting that the composite has reached a stable size. At these speeds, the sheer forces from agitation is inadequate to further fragment the composite. Furthermore, the Dv10 remains relatively unaffected by the increase in agitation speed. This indicates that the sheer forces required to fragment smaller composite are higher as compared to larger ones.

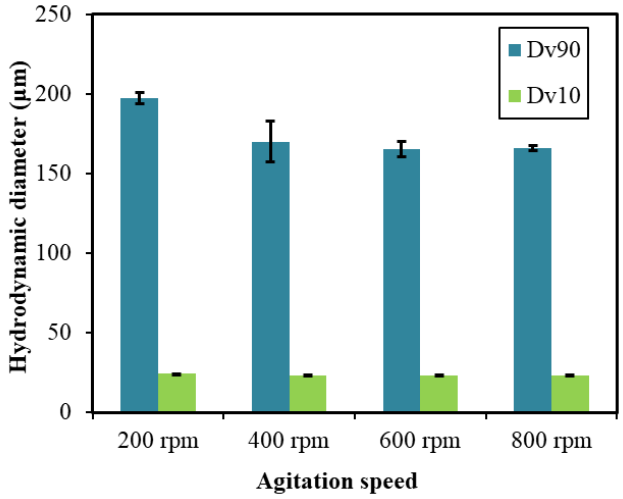

Figure 5. Effect of stirring speed on the particle size of TiO_2-A composite

Figure 6 shows the FT-IR spectrum for TiO_2-A composite, sodium alginate, and TiO_2 nanoparticles. The FT-IR analysis was performed to determine the presence of TiO_2 nanoparticles on TiO_2-A composite. The stretching of the protonated carboxylic group in the sodium alginate is shown at a wavenumber of 1592 cm^{-1} [33]. By comparing the spectrum of TiO_2-A composite and sodium alginate, the peak of the carboxylic group shifted from 1592 to 1602 cm^{-1}, indicating that there were interactions between the carboxylic group and TiO_2 nanoparticles. The interactions could be caused by the electrostatic interactions between negatively charged alginate polymer and positively charged TiO_2 nanoparticles. FT-IR spectra of TiO_2 nanoparticles consist of two characteristic features, i) observable peaks at wavenumber of 1610 and 3229 cm^{-1}, which correspond to the presence of physisorbed and chemisorbed water molecules on TiO_2 nanoparticles. The obtained results are consistent with those reported in the literature [34]; ii) characteristic band present over a wavenumber of 850 to 1250 cm^{-1}, which corresponds to the pattern of the O–Ti–O network reported in the literature [35,36]. From the

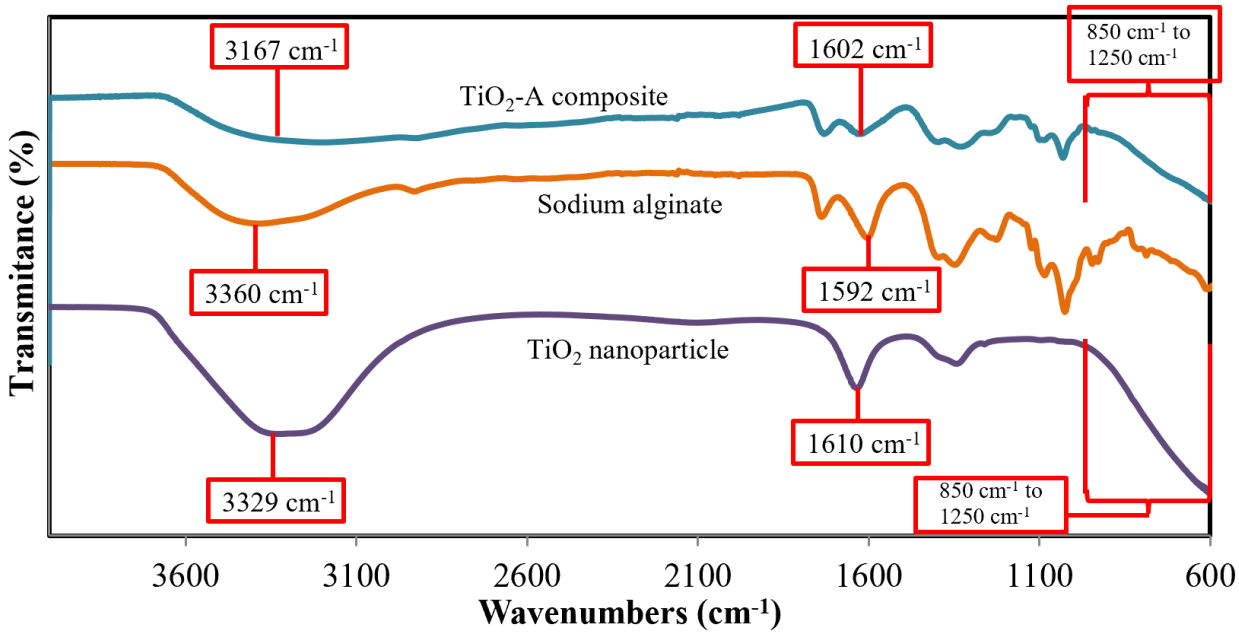

Figure 6. FT-IR spectrum of TiO_2-A composite, sodium alginate and TiO_2 nanoparticles.

spectra of TiO_2-A composite, the O–H stretching shifted from 3360 to 3176 cm^{-1} and the characteristic band present over a wavenumber of 850 to 1250 cm^{-1} of O–Ti–O network was also observed. The presence of both features on the spectra strongly suggests that the TiO_2 was immobilized and formed the TiO_2-A composite.

The FE-SEM micrographs of protonated alginate and TiO_2-A composite are shown in Figure 7. Figure 7(a) and (b) show the surface morphology of protonated alginate while Figure 7(c) and (d) show the surface morphology of TiO_2-A composite. As shown in Figure 7(a) and (c), the surface of the TiO_2-A composite is more porous (*i.e.* pores are indicated by yellow arrows) than the surface of protonated alginate. A rough surface was observed on the TiO_2-A composite [see Figure 7(d)], due to the presence of TiO_2 nanoparticles on the surface. The presence of TiO_2 on the surface of the TiO_2-A composite was further confirmed by EDX mapping, which shows the presence of titanium (Ti) element (indicated by white dots) on the Ti-map.

3.2 Photoactivity of the TiO_2-A Composite Photocatalyst

The photoactivity of TiO_2 nanoparticles and TiO_2-A composite were demonstrated using surrogate pollutants of RB5. Figure 8(a) presents the kinetic data for the removal of RB5 with TiO_2-A composite and TiO_2 nanoparticles with and without UV illumination. As shown in Figure 8(a) (i), the removal efficiency of RB5 by sole UV illumination is marginal (< 15% after 240 min).

The removal of RB5 with TiO_2-A composite was subsequently investigated without UV illumination [see Figure 8(a) (ii)]. No significant decrease in the concentration of RB5 was observed throughout the 240 min of the experiment. This indicates that there is limited adsorption of RB5 by TiO_2-A composite. Figure 8(a) (iii) shows the kinetic data of the removal of RB5 with TiO_2-A composite under UV illumination. More than 90% of RB5 was removed within 150 min of the UV illumination with the presence of TiO_2-A composite. Typically, the degradation kinetics of dye in an aqueous solution by photocatalysis follow a pseudo first-order kinetic model [37]. The kinetic data obtained for the TiO_2-A composite were fitted with this model. The plot shows a lag phase at the beginning of the photocatalysis reaction which could be a sign of restricted diffusion of RB5 through the alginate polymer to the surface of TiO_2. As the RB5 diffused continuously to the surface of TiO_2, the lag-phase disappeared and the degradation kinetics followed the first order kinetics with rate constant, k, of 0.022 and R^2 of 0.973 [see Figure 8(b)].

3.3 Effects of pH

pH is a crucial parameter that affects the photoactivity of TiO_2-A composite due to its effects on the surface charge of TiO_2 [38,39]. Generally, the surface charge of TiO_2 nanoparticle is dependent on the pH of the suspension, following the equilibria that describe the ionization state of TiO_2:

$$TiOH_2^+ \rightleftharpoons TiOH + H^+, \quad pH < pH_{PZC}$$

$$TiOH \rightleftharpoons TiO^- + H^+, \quad pH > pH_{PZC}$$

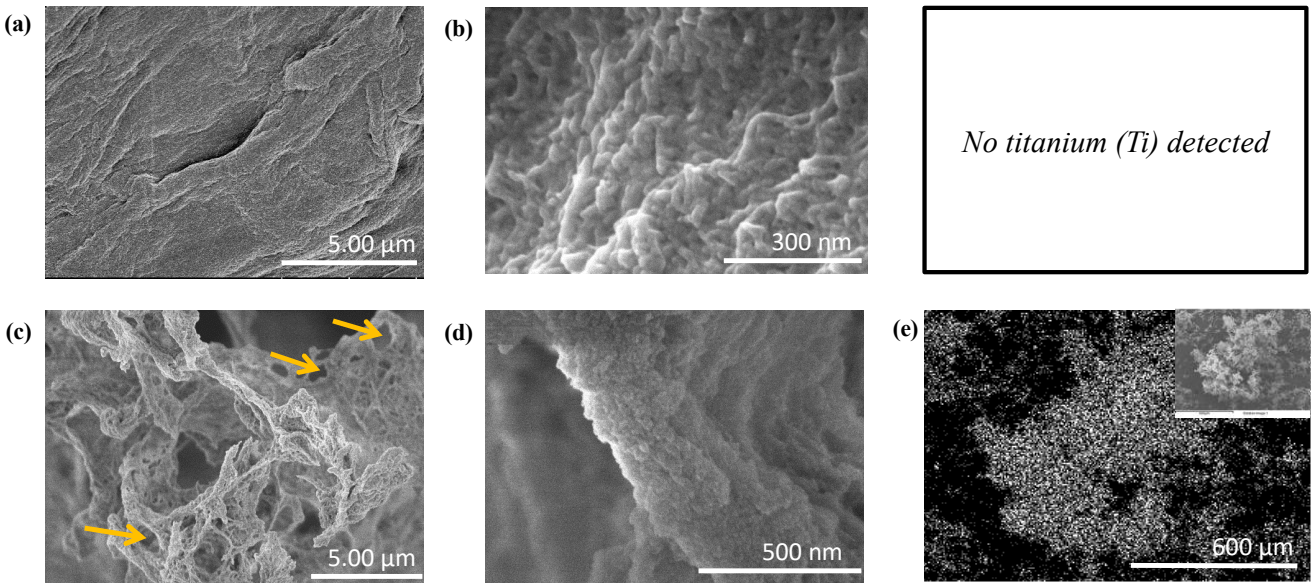

Figure 7. FE-SEM micrograph of protonated alginate at (a) low and (b) high magnification; FE-SEM micrograph of TiO_2-A composite at (c) low and (d) high magnification; (e) the EDX Ti-Map and the corresponding micrograph (inset). The pores observed in TiO_2-A composite are indicated with yellow arrows. The presence of titanium (Ti) in EDX mapping analysis is indicated by white dots.

RB5 is known to be negatively charged because of its sulfonic groups [40]. Therefore, the optimum pH for RB5 removal is lower than the pH_{PZC} of TiO_2, which is below the range of pH 4.6 to 6.9 [41,42]. The pH_{PZC} of TiO_2 used in this study was approximately pH 6.4 (see Figure 9). At pH 2, the negatively charged RB5 was strongly attracted to the positively charged TiO_2. As a result, more than 80% of the initial RB5 concentration was removed by TiO_2-A composite within 30 min (see Figure 10). When the pH was increased to 4, the TiO_2-A composite required approximately 140 min to achieve a similar removal capacity due to the reduced charged density of the composite. At pH 6 and above, the removal rate of the RB5 reduced further due to weak attraction between the composite and RB5.

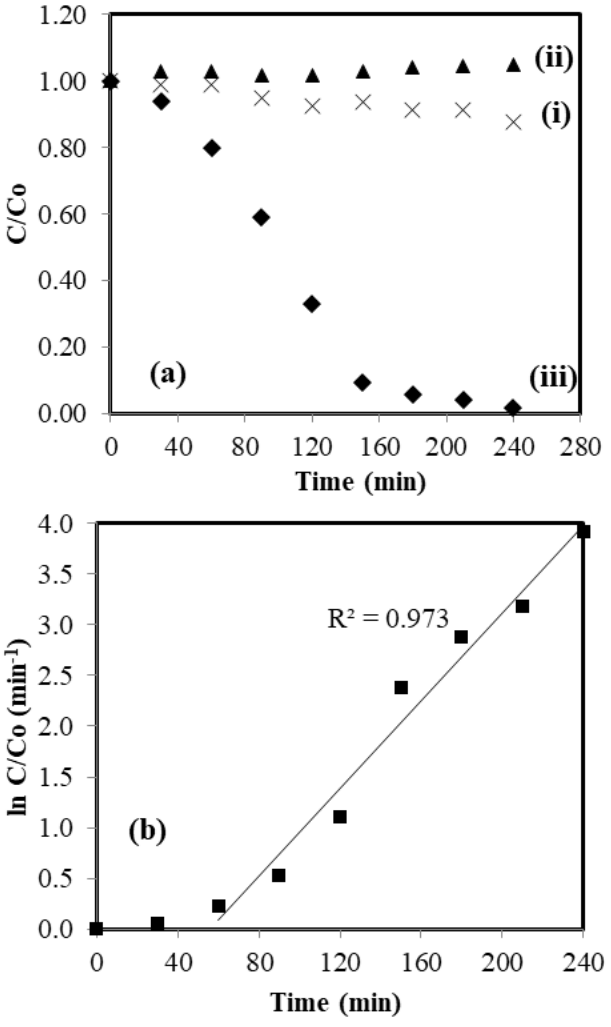

Figure 8. (a) Kinetic data for removal of RB5 by (i) solely UV illumination (×), TiO_2-A composite (ii) without UV illumination (▲), (iii) with UV illumination (♦) and (b) Kinetic data of RB5 removal with TiO_2-A composite represented using pseudo first-order kinetics; the initial RB5 concentration was 5 ppm with photocatalyst dosage of 0.01% (w/v). The initial pH of the experiments was maintained at pH = 4.

3.4 Recovery and Reusability of TiO_2-A Composite Photocatalyst

The TiO_2 nanoparticles and TiO_2-A composite were allowed to settle for 24 h after the photocatalytic experiments. Solid-liquid phase separation was observed for TiO_2-A composite while no phase separation was observed for TiO_2 nanoparticles suspension after 24 h. The results show that the composite could be easily separated through gravitational sedimentation. However, it is impossible to recover the TiO_2 nanoparticles through gravitational settling, thus confirming the difficulty in recovering TiO_2 nanoparticles using a simple separation method.

Subsequently, the reusability of TiO_2-A composite was tested for up to 10 process cycles (see Figure 11) to demonstrate its lifespan.

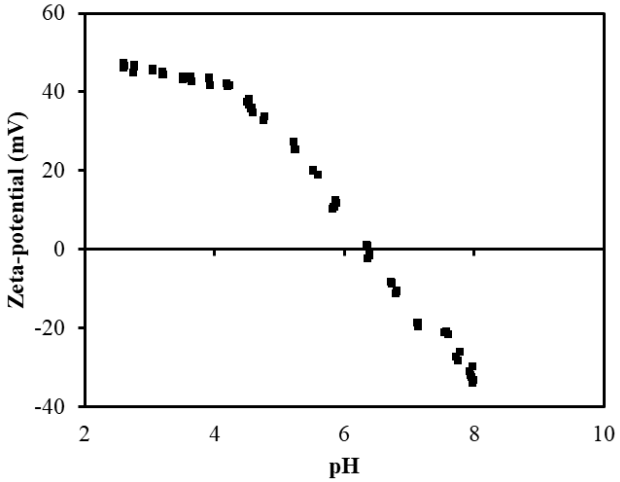

Figure 9. Potentiometric curve of TiO_2 nanoparticles suspension. The point of zero charge (PZC) of TiO_2 nanoparticles is approximately pH = 6.4.

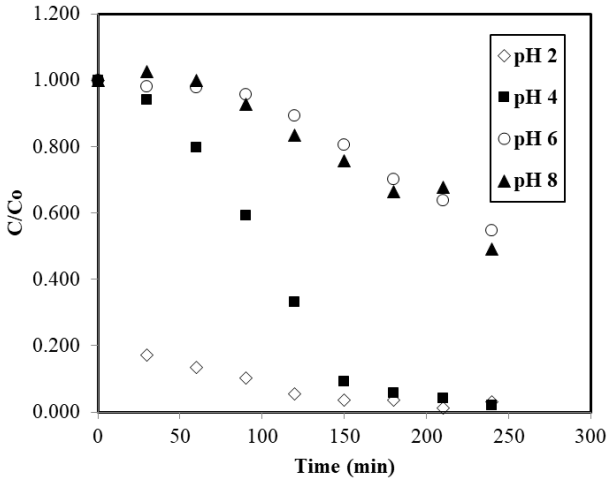

Figure 10. Kinetic data for removal of RB5 by TiO_2-A composite with UV illumination at various pH; the initial RB5 concentration was 5 ppm with photocatalyst dosage of 0.01% (w/v).

Throughout the 10 process cycles, all photocatalytic experiments were able to achieve a removal efficiency greater than 90% consistently. These results show that the composite has excellent performance during reuse and a long lifespan, which are important considerations for practical applications in wastewater treatment.

3.5 Comparison with Literatures

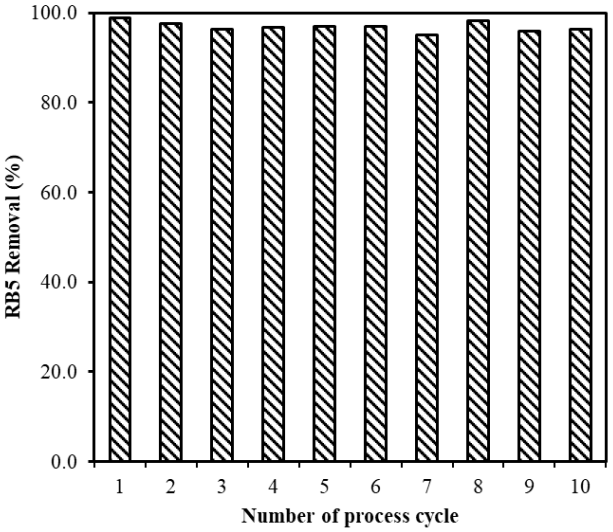

Figure 11. Reusability of TiO_2-A composite for 10 process cycles. The conditions of the experiments were maintained at an initial RB5 concentration of 5 ppm and 0.01 % (w/v) of TiO_2-A composite with reaction time fixed at 240 min. The initial pH of the experiments was maintained at pH = 4.

The TiO_2-A composite photocatalyst, synthesized via a facile and rapid immobilization technique, exhibited promising photodegradation capabilities compared to other studies utilizing alginate-based materials as sustainable immobilization supports (as presented in Table 1). This study demonstrates that the TiO_2-A composite achieved an 86.6% degradation of pollutants within 60 min, using a catalyst dosage of 0.1 g/L. This could be due to the particle size of the immobilized photocatalyst is significantly smaller as compared to other studies which is reported to be in millimetric size. It should be noted that various factors, such as catalyst dosage, pH, temperature, light intensity and the pollutant, could influence the photodegradation efficiency of the alginate-based TiO_2-based photocatalyst. Nonetheless, when compared to previous research utilizing alginate as a catalyst support, as shown in Table 1, the TiO_2-A composite demonstrated comparable or superior performance while utilizing a lower quantity of catalyst.

4. Conclusions

A facile and rapid approach to immobilize nano-sized TiO_2 with a renewable biopolymer, i.e. alginate, was demonstrated. The particle size analysis, TGA, EDX, and FTIR confirmed the immobilization of TiO_2 nanoparticles on the alginate polymer. The TiO_2-A composite was capable of removing RB5 by photocatalysis. More than 98% of the RB5 was removed within 4 h of

Table 1. Comparison of photocatalytic degradation with literature.

Catalyst	Catalyst dosage (g/L)	Pollutant	Initial pollutant concentration (ppm)	Degradation of pollutants after 120 mins (%)	Ref.
Floating TiO_2/ calcium alginate	1.0	Tartrazine	50	≈ 55	[43]
TiO_2/ alginate macrobead	20	Methylene Blue	32	≈ 25	[44]
	20	Methylene Blue	3.2	≈ 45	[44]
	100	Methyl Orange	33	100	[44]
	100	Methyl Orange	3.3	100	[44]
TiO_2/Cobalt cross-linked alginate	40	Methyl Orange	5	≈ 65	[45]
TiO_2/Copper cross-linked alginate	40	Methyl Orange	5	≈ 50	[45]
TiO_2/Strontium cross-linked alginate	40	Methyl Orange	5	95	[45]
TiO_2-A composite	0.1	Reactive Black 5	5	86.6	This work

UV illumination. The TiO_2-A composite gave a high degradation rate at low pH (pH < pH_{PZC}). In addition, the TiO_2-A composite can be easily recovered by gravitational sedimentation and showed a high removal rate (>90%) for up to 10 cycles of reuse. The TiO_2-A composite demonstrated comparable or superior photodegradation performance while utilizing a lower quantity of catalyst and is a promising immobilized photocatalyst for practical application in wastewater treatment.

Acknowledgments

This research is supported by the Ministry of Higher Education Malaysia through the Fundamental Research Grant Scheme (FRGS), project number (FRGS/1/2022/TK09/XMU/02/3). This research is also supported by the Xiamen University Malaysia Research Fund (XMUMRF) (Grant No: XMUMRF/2019-C4/IENG/0018).

CRediT Author Statement

Author Contributions: *W. H. Lam*: Conceptualization, Writing Draft Preparation, Methodology, Formal Analysis, Investigation; *L. H. Tee*: Writing, Review, and Editing; *Z. H. Ban*: Review and Editing. All authors have read and agreed to the published version of the manuscript.

References

[1] Nasralla, N.H.S., Yeganeh, M., Astuti, Y., Piticharoenphun, S., Šiller, L. (2018). Systematic study of electronic properties of Fe-doped TiO_2 nanoparticles by X-ray photoemission spectroscopy. *Journal of Materials Science: Materials in Electronics*, 29(20), 17956–17966. DOI: 10.1007/s10854-018-9911-5.

[2] Nasralla, N., Yeganeh, M., Astuti, Y., Piticharoenphun, S., Shahtahmasebi, N., Kompany, A., Karimipour, M., Mendis, B.G., Poolton, N.R.J., Šiller, L. (2013). Structural and spectroscopic study of Fe-doped TiO_2 nanoparticles prepared by sol–gel method. *Scientia Iranica*, 20(3), 1018–1022. DOI: 10.1016/j.scient.2013.05.017.

[3] Nemiwal, M., Zhang, T.C., Kumar, D. (2021). Recent progress in g-C_3N_4, TiO_2 and ZnO based photocatalysts for dye degradation: Strategies to improve photocatalytic activity. *Science of The Total Environment*, 767, 144896. DOI: 10.1016/j.scitotenv.2020.144896.

[4] Nur, A.S.M., Sultana, M., Mondal, A., Islam, S., Robel, F.N., Islam, A., Sumi, M.S.A. (2022). A review on the development of elemental and codoped TiO_2 photocatalysts for enhanced dye degradation under UV–vis irradiation. *Journal of Water Process Engineering*, 47, 102728. DOI: 10.1016/j.jwpe.2022.102728.

[5] González-Burciaga, L.A., Núñez-Núñez, C.M., Proal-Nájera, J.B. (2022). Challenges of TiO2 heterogeneous photocatalysis on cytostatic compounds degradation: state of the art. *Environmental Science and Pollution Research*, 29(28), 42251–42274. DOI: 10.1007/s11356-021-17241-8.

[6] Liu, Y., Xiang, Y., Xu, H., Li, H. (2022). The reuse of nano-TiO_2 under different concentration of CO_3^{2-} using coagulation process and its photocatalytic ability in treatment of methyl orange. *Separation and Purification Technology*, 282, 120152. DOI: 10.1016/j.seppur.2021.120152.

[7] Bathula, C., Rabani, I., Sekar, S., Youi, H.-K., Choy, J.-Y., Kadam, A., Shretha, N.K., Seo, Y.-S., Kim, H.-S. (2021). Enhanced removal of organic dye by activated carbon decorated TiO2 nanoparticles from Mentha Aquatica leaves via ultrasonic approach. *Ceramics International*, 47(6), 8732–8739. DOI: 10.1016/j.ceramint.2020.12.282.

[8] Lee, J., Seong, S., Jin, S., Jeong, Y., Noh, J. (2021). Synergetic photocatalytic-activity enhancement of lanthanum doped TiO_2 on halloysite nanocomposites for degradation of organic dye. *Journal of Industrial and Engineering Chemistry*, 100, 126–133. DOI: 10.1016/j.jiec.2021.05.029.

[9] Bahrudin, N.N. (2022). Evaluation of degradation kinetic and photostability of immobilized TiO2/activated carbon bilayer photocatalyst for phenol removal. *Applied Surface Science Advances*, 7, 100208. DOI: 10.1016/j.apsadv.2021.100208.

[10] Wang, X., Xuan, X., Wang, Y., Li, X., Huang, H., Zhang, X., Du, X. (2021). Nano-Au-modified TiO_2 grown on dendritic porous silica particles for enhanced CO_2 photoreduction. *Microporous and Mesoporous Materials*, 310, 110635. DOI: 10.1016/j.micromeso.2020.110635.

[11] Ji, H., Liu, W., Sun, F., Huang, T., Chen, L., Liu, Y., Qi, J., Xie, C., Zhao, D. (2021). Experimental evidences and theoretical calculations on phenanthrene degradation in a solar-light-driven photocatalysis system using silica aerogel supported TiO_2 nanoparticles: Insights into reactive sites and energy evolution. *Chemical Engineering Journal*, 419, 129605. DOI: 10.1016/j.cej.2021.129605.

[12] Suárez, S., Jansson, I., Ohtani, B., Sánchez, B. (2019). From titania nanoparticles to decahedral anatase particles: Photocatalytic activity of TiO2/zeolite hybrids for VOCs oxidation. *Catalysis Today*, 326, 2–7. DOI: 10.1016/j.cattod.2018.09.004.

[13] Munguti, L.K., Dejene, F.B., Muthee, D.K. (2023). Zeolite Na-A supported TiO_2: Effects of TiO_2 loading on structural, optical and adsorption properties. *Materials Science and Engineering: B*, 289, 116281. DOI: 10.1016/j.mseb.2023.116281.

[14] Wu, A., Wang, D., Wei, C., Zhang, X., Liu, Z., Feng, P., Ou, X., Qiang, Y., Garcia, H., Niu, J. (2019). A comparative photocatalytic study of TiO_2 loaded on three natural clays with different morphologies. *Applied Clay Science*, 183, 105352. DOI: 10.1016/j.clay.2019.105352.

[15] Dlamini, M.C., Maubane-Nkadimeng, M.S., Moma, J.A. (2021). The use of TiO_2/clay heterostructures in the photocatalytic remediation of water containing organic pollutants: A review. *Journal of Environmental Chemical Engineering*, 9(6), 106546. DOI: 10.1016/j.jece.2021.106546.

[16] Sandhu, S., Krishnan, S., Karim, A. V, Shriwastav, A. (2020). Photocatalytic denitrification of water using polystyrene immobilized TiO_2 as floating catalyst. *Journal of Environmental Chemical Engineering*, 8(6), 104471. DOI: 10.1016/j.jece.2020.104471.

[17] El-Mekkawi, D.M., Abdelwahab, N.A., Mohamed, W.A.A., Taha, N.A., Abdel-Mottaleb, M.S.A. (2020). Solar photocatalytic treatment of industrial wastewater utilizing recycled polymeric disposals as TiO_2 supports. *Journal of Cleaner Production*, 249, 119430. DOI: 10.1016/j.jclepro.2019.119430.

[18] Ali, H.M., Arabpour Roghabadi, F., Ahmadi, V. (2023). Solid-supported photocatalysts for wastewater treatment: Supports contribution in the photocatalysis process. *Solar Energy*, 255, 99–125. DOI: 10.1016/j.solener.2023.03.032.

[19] Kandathil, V., Kempasiddaiah, M., B. S., S., Patil, S.A. (2019). From agriculture residue to catalyst support; A green and sustainable cellulose-based dip catalyst for CC coupling and direct arylation. *Carbohydrate Polymers*, 223, 115060. DOI: 10.1016/j.carbpol.2019.115060.

[20] Musa, Y., Bwatanglang, I.B. (2020). Chapter 6 - Current role and future developments of biopolymers in green and sustainable chemistry and catalysis. In: Mohammad, F., Al-Lohedan, H.A., Jawaid, M. (eds) *Sustainable Nanocellulose and Nanohydrogels from Natural Sources*. Elsevier, pp. 131–154. DOI: 10.1016/B978-0-12-816789-2.00006-7.

[21] Mohd Adnan, M.A., Phoon, B.L., Muhd Julkapli, N. (2020). Mitigation of pollutants by chitosan/metallic oxide photocatalyst: A review. *Journal of Cleaner Production*, 261, 121190. DOI: 10.1016/j.jclepro.2020.121190.

[22] Liu, G., Pan, X., Li, J., Li, C., Ji, C. (2021). Facile preparation and characterization of anatase TiO_2/nanocellulose composite for photocatalytic degradation of methyl orange. *Journal of Saudi Chemical Society*, 25(12), 101383. DOI: 10.1016/j.jscs.2021.101383.

[23] Balakrishnan, A., Appunni, S., Chinthala, M., Vo, D.-V.N. (2022). Biopolymer-supported TiO_2 as a sustainable photocatalyst for wastewater treatment: a review. *Environmental Chemistry Letters*, 20(5), 3071–3098. DOI: 10.1007/s10311-022-01443-8.

[24] Dalponte Dallabona, I., Mathias, Á.L., Jorge, R.M.M. (2021). A new green floating photocatalyst with Brazilian bentonite into TiO_2/alginate beads for dye removal. *Colloids and Surfaces A: Physicochemical and Engineering Aspects*, 627, 127159. DOI: 10.1016/j.colsurfa.2021.127159.

[25] Isik, Z., Bilici, Z., Adiguzel, S.K., Yatmaz, H.C., Dizge, N. (2019). Entrapment of TiO_2 and ZnO powders in alginate beads: Photocatalytic and reuse efficiencies for dye solutions and toxicity effect for DNA damage. *Environmental Technology & Innovation*, 14, 100358. DOI: 10.1016/j.eti.2019.100358.

[26] Shehzad, H., Ahmed, E., Sharif, A., Farooqi, Z.H., Din, M.I., Begum, R., Liu, Z., Zhou, L., Ouyang, J., Irfan, A., Nawaz, I. (2022). Modified alginate-chitosan-TiO_2 composites for adsorptive removal of Ni(II) ions from aqueous medium. *International Journal of Biological Macromolecules*, 194, 117–127. DOI: 10.1016/j.ijbiomac.2021.11.140.

[27] El-Sheekh, M.M., Deyab, M.A., Hassan, N.I., Abu Ahmed, S.E. (2022). Green biosynthesis of silver nanoparticles using sodium alginate extracted from Sargassum latifolium and their antibacterial activity. *Rendiconti Lincei Scienze Fisiche e Naturali*, 33(4), 867–878. DOI: 10.1007/s12210-022-01102-8.

[28] La Zara, D., Bailey, M.R., Hagedoorn, P.-L., Benz, D., Quayle, M.J., Folestad, S., van Ommen, J.R. (2020). Sub-nanoscale Surface Engineering of TiO_2 Nanoparticles by Molecular Layer Deposition of Poly(ethylene terephthalate) for Suppressing Photoactivity and Enhancing Dispersibility. *ACS Applied Nano Materials*, 3(7), 6737–6748. DOI: 10.1021/acsanm.0c01158.

[29] Paşcalău, V., Popescu, V., Popescu, G.L., Dudescu, M.C., Borodi, G., Dinescu, A., Perhaiţa, I., Paul, M. (2012). The alginate/k-carrageenan ratio's influence on the properties of the cross-linked composite films. *Journal of Alloys and Compounds*, 536, S418–S423. DOI: 10.1016/j.jallcom.2011.12.026.

[30] Wang, S., Huang, X., Elimelech, M. (2020). Complexation between dissolved silica and alginate molecules: Implications for reverse osmosis membrane fouling. *Journal of Membrane Science*, 605, 118109. DOI: 10.1016/j.memsci.2020.118109.

[31] AlShammari, A.S., Halim, M.M., Yam, F.K., Kaus, N.H.M. (2020). Synthesis of Titanium Dioxide (TiO_2)/Reduced Graphene Oxide (rGO) thin film composite by spray pyrolysis technique and its physical properties. *Materials Science in Semiconductor Processing*, 116, 105140. DOI: 10.1016/j.mssp.2020.105140.

[32] Ong, W.-J., Tan, L.-L., Chai, S.-P., Yong, S.-T., Mohamed, A.R. (2014). Self-assembly of nitrogen-doped TiO_2 with exposed {001} facets on a graphene scaffold as photo-active hybrid nanostructures for reduction of carbon dioxide to methane. *Nano Research*, 7(10), 1528–1547. DOI: 10.1007/s12274-014-0514-z.

[33] Pathak, T., Kim, J., Lee, S.-J., Baek, D.-J., Paeng, K.-J. (2008). Preparation of Alginic Acid and Metal Alginate from Algae and their Comparative Study. *Journal of Polymers and the Environment*, 16(3), 198–204. DOI: 10.1007/s10924-008-0097-4.

[34] Tryba, B., Rychtowski, P., Srenscek-Nazzal, J., Przepiorski, J. (2020). The inflence of TiO_2 structure on the complete decomposition of acetaldehyde gas. *Materials Research Bulletin*, 126, 110816. DOI: 10.1016/j.materresbull.2020.110816.

[35] García-Contreras, L.A., Flores-Flores, J.O., Arenas-Alatorre, J.Á., Chávez-Carvayar, J.Á. (2022). Synthesis, characterization and study of the structural change of nanobelts of TiO_2 ($H_2Ti_3O_7$) to nanobelts with anatase, brookite and rutile phases. *Journal of Alloys and Compounds*, 923, 166236. DOI: 10.1016/j.jallcom.2022.166236.

[36] Zare, M.H., Mehrabani-Zeinabad, A. (2022). Photocatalytic activity of $ZrO_2/TiO_2/Fe_3O_4$ ternary nanocomposite for the degradation of naproxen: characterization and optimization using response surface methodology. *Scientific Reports*, 12(1), 10388. DOI: 10.1038/s41598-022-14676-y.

[37] Tekin, D., Kiziltas, H., Ungan, H. (2020). Kinetic evaluation of ZnO/TiO_2 thin film photocatalyst in photocatalytic degradation of Orange G. *Journal of Molecular Liquids*, 306, 112905. DOI: 10.1016/j.molliq.2020.112905.

[38] Tichapondwa, S.M., Newman, J.P., Kubheka, O. (2020). Effect of TiO_2 phase on the photocatalytic degradation of methylene blue dye. *Physics and Chemistry of the Earth, Parts A/B/C*, 118–119, 102900. DOI: 10.1016/j.pce.2020.102900.

[39] Upadhyay, G.K., Rajput, J.K., Pathak, T.K., Swart, H.C., Purohit, L.P. (2020). Photoactive $CdO:TiO_2$ nanocomposites for dyes degradation under visible light. *Materials Chemistry and Physics*, 253, 123191. DOI: 10.1016/j.matchemphys.2020.123191.

[40] Yang, K., Liu, Y., Li, Y., Cao, Z., Zhou, C., Wang, Z., Zhou, X., Baig, S.A., Xu, X. (2019). Applications and characteristics of Fe-Mn binary oxides for Sb(V) removal in textile wastewater: Selective adsorption and the fixed-bed column study. *Chemosphere*, 232, 254–263. DOI: 10.1016/j.chemosphere.2019.05.194.

[41] Phuinthiang, P., Kajitvichyanukul, P. (2018). Degradation of paraquat from contaminated water using green TiO_2 nanoparticles synthesized from Coffea arabica L. in photocatalytic process. *Water Science and Technology*, 79(5), 905–910. DOI: 10.2166/wst.2018.493.

[42] Liu, M., Yin, W., Qian, F.-J., Zhao, T.-L., Yao, Q.-Z., Fu, S.-Q., Zhou, G.-T. (2020). A novel synthesis of porous TiO_2 nanotubes and sequential application to dye contaminant removal and Cr(VI) visible light catalytic reduction. *Journal of Environmental Chemical Engineering*, 8(5), 104061. DOI: 10.1016/j.jece.2020.104061.

[43] Dalponte, I., de Sousa, B.C., Mathias, A.L., Jorge, R.M.M. (2019). Formulation and optimization of a novel TiO_2/calcium alginate floating photocatalyst. *International Journal of Biological Macromolecules*, 137, 992–1001. DOI: 10.1016/j.ijbiomac.2019.07.020.

[44] Gjipalaj, J., Alessandri, I. (2017). Easy recovery, mechanical stability, enhanced adsorption capacity and recyclability of alginate-based TiO_2 macrobead photocatalysts for water treatment. *Journal of Environmental Chemical Engineering*, 5(2), 1763–1770. DOI: 10.1016/j.jece.2017.03.017.

[45] Wan, S., Zhao, W., Xiong, D., Li, S., Ye, Y., Du, L. (2022). Novel alginate immobilized TiO_2 reusable functional hydrogel beads with high photocatalytic removal of dye pollutions. *Journal of Polymer Engineering*, 42(10), 978–985. DOI: 10.1515/polyeng-2022-0017.